JOURNAL OF Applied Polymer SCIENCE

Free-Standing Aniline Oligomer Functionalized Multiwalled Carbon Nanotube Films from a Filtration Method

Qiguan Wang, Wei Zhou, Sumin Wang, Jianping Li, Wenzhi Zhang, Xiaomin Wang

Scientific Research Innovation Team of Solidification Theory and Functional Materials, Shaanxi Key Laboratory of Photoelectric Functional Materials and Devices, School of Materials and Chemical Engineering, Xi'an Technological University, Xi'an 710021, People's Republic of China

Correspondence to: S. M. Wang (E-mail: suminwang@163.com)

ABSTRACT: High electrochemical active free-standing multiwalled carbon nanotube (MWNT) films have been synthesized from aniline oligomer functionalized MWNTs (MWNT-AO), by using filtration of the acidic phosphate ester (APE) doped MWNT-AO dispersions. The homogeneously distributed MWNTs endowed APE/MWNT films automatically releasing from the filter membrane. The sheet resistivity of MWNT-AO (850 Ω sq^{-1}) showed a lower value than that of carboxyl MWNTs (1273 Ω sq^{-1}), due to the doping effect of MWNT on aniline oligomer, confirmed by the N1s X-ray photoelectron spectrum. However, it showed a higher sheet resistivity value of 1526 Ω sq^{-1} after further doped by APE, because of the presence of unreacted dopant. After removing the residual insulating dopant by the vacuum filtration, the resultant APE/MWNT films showed the sheet resistivity value as low as 131 Ω sq^{-1}. Thermogravimetric analysis showed that the MWNT loading in the film can be over than 77%, which showed the specific capacitance as high as 249 F g^{-1}. © 2013 Wiley Periodicals, Inc. J. Appl. Polym. Sci. **2014**, *131*, 40259.

KEYWORDS: anilline oligomer; multi-walled carbon nanotube film; filtration method

Received 30 October 2013; accepted 3 December 2013

DOI: 10.1002/app.40259

INTRODUCTION

As the promising materials applied potentially in novel electronic devices and energy-storage devices, substantive work has been carried out on the free-standing carbon nanotube (CNT) films.[1–4] CNT films are usually prepared by the dry methods of chemical vapor deposition (CVD)[5,6] and the wet methods based on the solution coating[7,8] and the vacuum filtrating processes.[9–11] In comparison with the CVD method at a relatively high temperature, the wet process of filtrating noncovalent wrapping CNTs has been extensively investigated, because of the simple, low-temperature manipulation. However, the CNT film from this method is typically fragile due to the re-clustering of CNTs after surfactant removing, which is difficult to transfer issue. Therefore, preparation of free-standing films easily released from the filter membranes by the filtration method is still a challenging task.

Polyaniline (PANI) is one of the most important conducting polymers due to its relatively easy processability, high-electrical conductivity, and environmental stability.[12,13] Polyaniline in the insulating emeraldine base form can be rendered conducting through protonation of the imine nitrogen sites with the protonic acid or through the charge transfer reaction,[14] which are generally known as the doping process. In addition, by using a suitably functionalized protonic acid to dope PANI, the counter ion can induce processability of the resulting PANI complex.[15] Over the past decade, tremendous efforts have been made to prepare CNT/PANI composites with an aim to synergistically combine the merits of each individual component.[16,17] Noncovalent wrapping[18,19] and covalent grafting[20] of CNTs are the mainly used strategies to achieve those composites. In comparison with the noncovalent wrapping CNT/PANI, the covalent grafting composites showed a more homogeneously distributed morphology due to the better solubility at the same CNT loading. By using counter-ion induced processability of conducting PANI complex, coupled with the covalent grafting method, it was reported that a water soluble self-doped CNT/sulfonic PANI composite with 17 wt % of CNTs was obtained,[21] which opened the possibility to prepare free-standing CNT films showing high strength, because the covalent attachment of PANI on CNT surfaces can effectively hinder the re-clustering of CNTs during the film formation. However, compared with the conducting PANI, this composite showed a low-electrical conductivity (5.6×10^{-3} S cm^{-1}) mainly because of the presence of strong electron-withdrawing substituted groups on PANI backbone as well as the low content of CNT loading.

Considering the surprisingly high-electrical conductivity of CNTs,[22] to assure the system has a high-CNT loading for

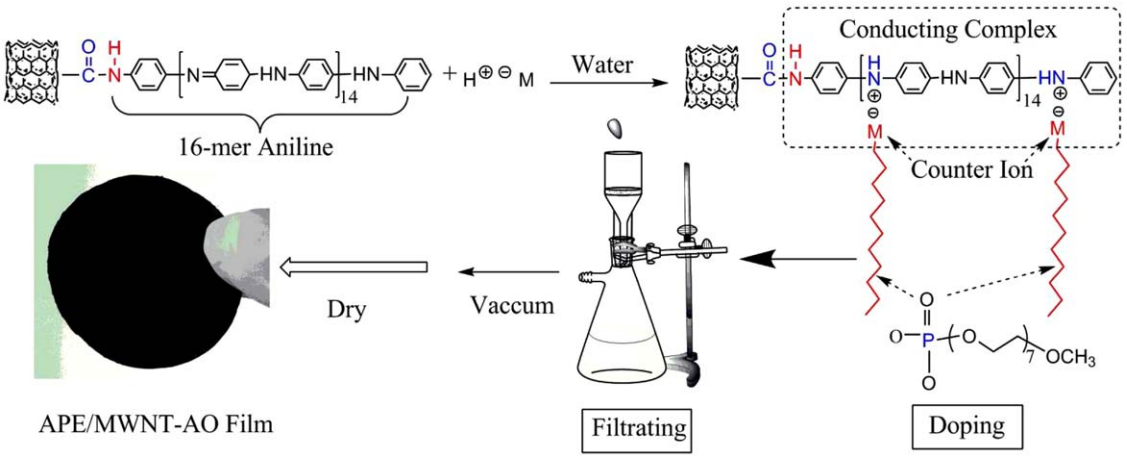

Figure 1. Illustration of the doping–filtrating process and the photographs of the as-prepared MWNT film. [Color figure can be viewed in the online issue, which is available at wileyonlinelibrary.com.]

getting the high-electrical conductivity, a PANI oligomer with the similar doping behavior as the high-molecular PANI was here attempted to covalently decorate the multiwalled carbon nanotube (MWNT), as shown in Figure 1. Under the counter-ion induced processability, a stable MWNT dispersion was obtained by doping the PANI oligomer with an organic protonic acid having a long tail. Furthermore, to remove the excess insulating dopant, a filtration process was proposed, which ensured the resultant CNT films showed the maximum electrical conductivity. Compared with the neat CNT, the covalent attachment of the conducting PANI units on the CNT sheet can hinder the re-clustering of CNTs, which may improve the strength of the resulting free-standing film and make it transfer easy. In addition, CNTs have been recognized as a potential electrode material for supercapacitors[23] due to their unique properties and nanometer size. Unfortunately, specific capacitance of CNT electrode usually ranges from 10 to 80 F g^{-1}.[24] Recently, the combination of conductive polymers showing high-redox pseudocapacitance with CNTs has been reported as an effective way to improve the specific capacitance of CNT electrode.[25] Therefore, the attachment of PANI units on CNT sheet may be expected to further endow the system excellent capacitance.

EXPERIMENTAL

Materials

Carboxylic acid functionalized MWNTs were purchased from Timesnano, Chengdu Organic Chemicals Co. Ltd., Chinese Academy of Sciences (>99% purity, length 10–20 μm). The —COOH content is approximately 0.5 wt %, measured by X-ray photoelectron spectrum (XPS) and titration methods. The *N*-phenyl-1,4-phenylenediamine used was obtained from Sigma-Aldrich (United States). Poly(ethylene glycol monomethyl ether)−350 (PEGME-350, where 350 is the average molecular weight of the ether oligomer) were of analytical purity purchased from Acros Co. $POCl_3$ and $SOCl_2$ were used after distillation (the $POCl_3$ and $SOCl_2$ solution are both highly corrosive, and therefore extreme care had to be exercised during handling). All other chemicals used were of analytical grade and used without further purification.

Preparation of Aniline Oligomers Endcapped with Amine Groups

Following the Zhang et al.[26] method, the oligomer of 16-mer aniline with a terminated amine group at one end was prepared from tetramer aniline, which was synthesized from the suspension reaction of *N*-phenyl-1,4-phenylenediamine with ferric chloride hexahydrate in 0.1*M* HCl solution. After dedoped by 0.1*M* ammonia hydroxide, the obtained emeraldine oligomers were recrystallized from ethanol.

Covalent Functionalization of MWNTs by Aniline Oligomers

As a typical example, 10 mg of MWNTs-COOH were firstly chlorinated by refluxing for 12 h with 20 mL of $SOCl_2$ at 70°C. After evaporating any remaining $SOCl_2$, aniline oligomer functionalized MWNTs (MWNT-AO) were then synthesized by reaction with 0.1 g of 16-mer aniline in dehydrated *N,N*-dimethyl formamide (DMF) for 24 h at 80°C. The resultant black powders were obtained after filtration and thoroughly rinsed by using DMF, acetone, and dried at 50°C in vacuum for 24 h.

Preparation of Organic Protonic Dopant

The organic protonic dopant of acidic phosphate ester (APE) was synthesized from the reaction of $POCl_3$ (0.5 mol) and PEGME-350 (1.0 mol) under vigorous stirring at 65°C for 24 h under nitrogen.[12] The residual water was removed in vacuum at 70°C for 2 h, and the product was further dried over 4 Å molecular sieves for 2 days prior to use. The acidity value of APE determined by potentiometric titration was 1.8×10^{-3} mol mL^{-1}.

Doping of Aniline Oligomer Functionalized MWNTs

Doping of MWNT-AOs was realized by exposure to protonic acid of APE. As shown in Figure 1, 16-mer aniline was doped to be conducting through protonation of the imine nitrogen sites by the protonic acid APE (H^+M^-) according to the acid–base chemistry. The formed counter ion (M^-) having the long tail of PEG endowed the APE/MWNT-AO system good solubility besides ensuring overall charge neutrality. The APE/MWNT-AO complex was formed by mixing 10 mg of MWNT-AO and

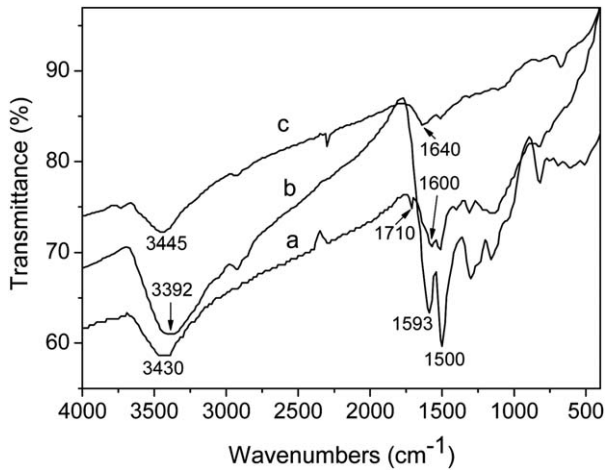

Figure 2. FT-IR spectra of (**a**) MWNT-COOH, (**b**) Aniline oligomer of 16-mer, and (**c**) MWNT-AO.

80 mg of APE at room temperature under vigorous stirring for 1 h. Followed by adding 4 mL of distilled water and then stirred at 50°C for 2 h, stable dispersions of APE/MWNT-AO caused by the counter-ion induced processability from APE were obtained. The molar ratio of H^+ in APE to phN- in oligomer was over than 0.5 to assure complete doping of aniline oligomer.

Free-Standing APE/MWNT-AO Films from Filtrating

In order to remove the excess insulating APE and lead to high-electrical conductivity, the APE/MWNT-AO dispersions were filtrated by using polycarbonates membrane filter (0.2 μm),[27] and then thoroughly washed with large quantity of distilled water. After drying at 50°C in vacuum oven for 12 h, free-standing APE/MWNT-AO films automatically released from the filter membranes were obtained, as illustrated from the photograph in Figure 1.

Electrochemical Measurements

The electrochemical measurements were conducted by using coin-type test cell (CR2032) with stainless steel working as both counter and reference electrode. The working electrodes were prepared by the following steps: 85 wt % active materials (MWNT or MWNT-COOH), 15 wt % acetylene black, and 5 wt % binder (polyvinylidene fluoride [PVDF]) were blended with *N*-methylpyrrolidone as a solvent. Electrode film was prepared by coating the mixture on a stainless steel mesh with diameter of 16 mm and dried successively in a vacuum oven at 120°C for 12 h. A Celgard 2400 polypropylene membrane was used as the separator. 1.0*M* H_2SO_4 solution was used as the electrolyte. For the fabrication of APE/MWNT-AO electrode, the APE/MWNT-AO film supported on the stainless steel mesh was directly sealed in the test cell.

Characterization

The functionalization of MWNTs was monitored by using a Fourier transform infrared (FT-IR) spectrometer (Nicolet Magna-IR 750) employing the KBr disk method. The sheet chemistry of functionalized MWNTs was analyzed using a Kratos AXIS 165 X-ray photoelectron spectrometer. All spectra were calibrated with the C1s photoemission peak for sp^2 hybridized carbons at 284.5 eV. Curve fitting of the photoemission spectra was done after a Shirley type background subtraction. Sheet resistances were measured by using a standard four-point probe configuration. Sheet morphology and interior structure of MWNT films were investigated using a scanning electron microscope (JEOL S-4800 SEM) operating at 10.0 kV. Morphologies of the functionalized MWNTs were recorded on a JEOL JEM-2010 microscope. For the transmission electron microscope (TEM) experiments, an appropriate amount of the samples suspended in distilled water was ultrasonicated for 30 min before being poured onto carbon-coated copper TEM grids. Thermogravimetric analysis (TGA) was obtained using the METTLER thermal analysis system under nitrogen atmosphere at a heating rate of 10°C min^{-1}. The X-ray diffraction (XRD) patterns of the samples were recorded with a Japan Shimadzu XRD-6000 X-ray diffractometer. The Cu$K\alpha$ line ($\lambda = 1.5451$ nm) from a sealed tube with a copper anode was used as a source of radiation. Galvanostatic charge/discharge tests were performed on Neware CT3008W (China) at a current density of 1.0 A g^{-1} with the potential between 0.08 and 0.8 V.

RESULTS AND DISCUSSION

FT-IR of MWNT-AO

The FT-IR spectra of the MWNT-AO were obtained to investigate the functionalization formed on MWNTs, as illustrated in Figure 2. From the spectrum of the MWNT-COOH [Figure 2(a)], it can be seen the peak occurring at 1710 cm^{-1} was assigned to the C═O stretching mode of the ─COOH groups from the MWNT backbone, and the intense broad peak centered at 3430 cm^{-1} was assigned to the ─OH stretching mode of the ─COOH group.[28,29] Two major bands at 1593 and 1500 cm^{-1}, respectively, corresponding to quinone ring deformation and benzene ring C═C stretching deformation in pure 16-mer aniline were observed [Figure 2(b)]. The wide band centered at 3392 cm^{-1} attributed to the amine groups showed the resultant 16-mer aniline was endcapped by amine,[26] which can be coupled with MWNT-COOH to form amide bond through acylation and amidation. From the spectrum of the MWNT-AO [Figure 2(c)], the peak observed at 3445 cm^{-1} was assigned to the NH stretching mode of the amide (─NHCO─) group, accompanied by the characteristic wide peak located at

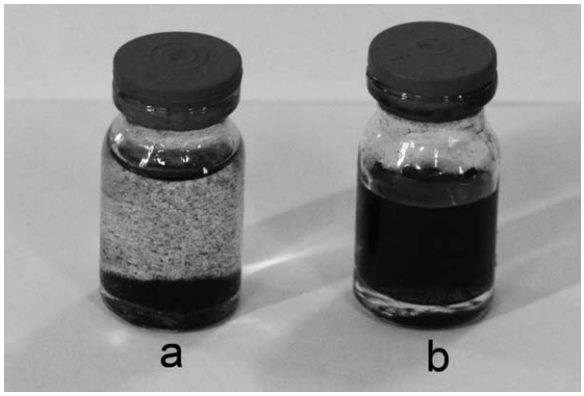

Figure 3. Photographs of dispersions of (**a**) MWNT-COOH and (**b**) MWNT-AO doped by APE in deionized water for 2 days standing.

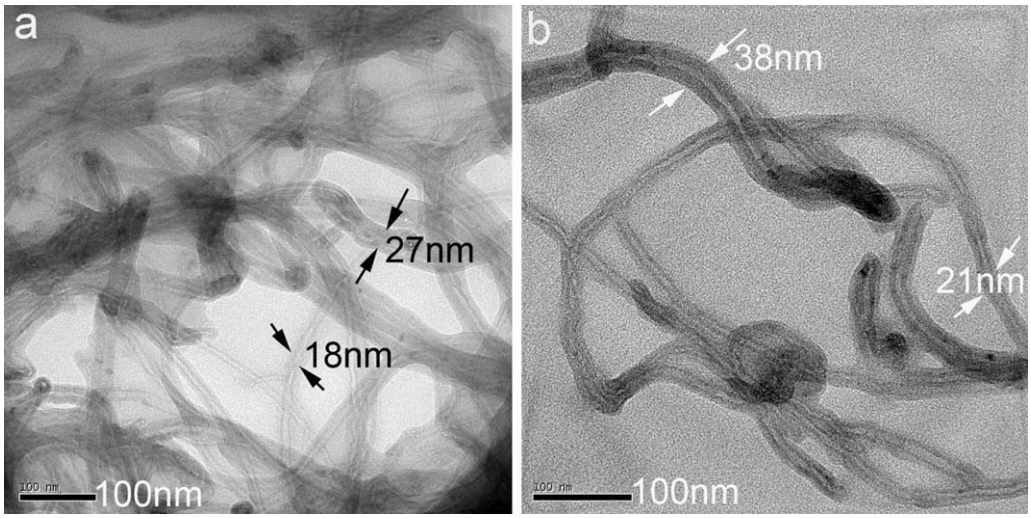

Figure 4. TEM images of (**a**) MWNT-COOH and (**b**) MWNT-AO.

1640 cm^{-1} corresponding to stretching of C═O groups, which showed the aniline oligomer was successfully grafted on the MWNTs by amide bonds.[30] Notably, the bands at 1593 and 1500 cm^{-1} in 16-mer aniline are not visible in the FT-IR spectra of MWNT-AO, because of the overlapping absorption from MWNTs at the same wave numbers. The successful functionalization of MWNTs by aniline oligomer supports the possibility to form APE/MWNT-AO complex through the doping process, which can be dispersed in water under the counter-ion induced processability of APE.

Stability of APE/MWNT-AO Dispersions

Due to the counter-ion induced processability from APE, MWNT-AO was dispersed stably in water. In comparison with MWNT-COOH, the resultant APE/MWNT-AO dispersion was more homogeneously distributed, as confirmed from Figure 3(a,b). Achieving the dispersion of MWNT-COOH into water was very difficult even after the CNTs were sonicated. As illustrated from Figure 3(a), it is clear that MWNT-COOH is insoluble in water, and there was much sedimentation at the bottom of the vial. However, the MWNT-AO doped by APE is soluble in water to form a homogeneous dispersion [Figure 3(b)] because of the strong counter-ion induced processability mainly resulted from the PEG chain on APE, showing no precipitation even after 2 days. The better solubility of APE/MWNT-AO can make the obtained films possess a satisfied strength for the easy releasing from the supporting substrate.

TEM Images

In order to detect the morphological changes of MWNTs upon modification, TEM experiences were performed. As shown in Figure 4(a), the average diameter of MWNT-COOH was about 18 nm, with the maximum value of 27 nm. However, after attached by 16-mer aniline, the average diameter shown in Figure 4(b) was increased to 21 nm, and the maximum value was also increased to 38 nm. This is because of the sheet deposition of 16-mer aniline layer on MWNT-COOH. In addition, the wrapping of MWNTs by aniline oligomer was seen to be very tight from the smooth features, probably owing to the presence of strong π–π interactions between such two components.

XRD Analysis

Figure 5 shows typical XRD patterns of the as-prepared 16-mer aniline, MWNT-COOH, and MWNT-AO powder. Two weak characteristic Bragg diffraction peaks of PANI are found at $2\theta = 20°$ and 23° for 16-mer aniline powder [Figure 5(a)], which showed that the crystallinity of the samples is very low.[31] For MWNT-COOH [Figure 5(b)], the sharp diffraction peak with strong intensity at $2\theta = 26°$ was assigned to (002) reflections, and the weak wide diffraction peak with strong intensity at $2\theta = 43°$ was attributed to (101) reflections.[32] Moreover, decorated by aniline oligomer, the two characteristic Bragg diffraction peaks of MWNT-AO were similar to those of MWNT-COOH, which indicated the periodic arrangement of carbon atoms in MWNT was not further disturbed by the attachment

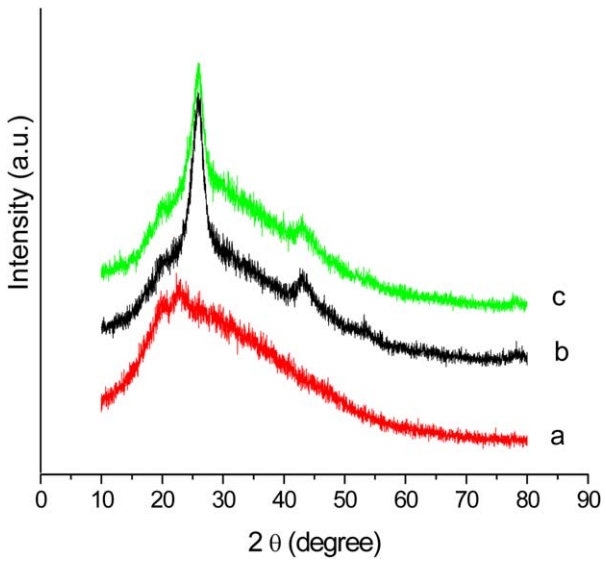

Figure 5. XRD patterns of (**a**) 16-mer aniline, (**b**) MWNT-COOH, and (**c**) MWNT-AO. [Color figure can be viewed in the online issue, which is available at wileyonlinelibrary.com.]

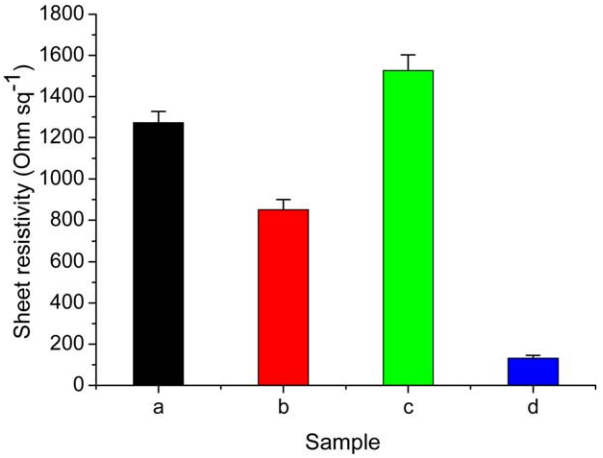

Figure 6. Sheet resistivity of (**a**) MWNT-COOH, (**b**) MWNT-AO, (**c**) solution casting APE/MWNT-AO films, and (**d**) APE/MWNT-AO films after filtrated. [Color figure can be viewed in the online issue, which is available at wileyonlinelibrary.com.]

of aniline oligomer. This assures the structures and properties of MWNT-COOH keep intact prior to use.

Electrical Conductivities

To investigate the effects of aniline units on the electrical conductivity, the sheet resistivity of MWNT-AO was measured. From Figure 6, it can be seen the sheet resistivity of MWNT-COOH is around 1273 Ω sq^{-1} (Sample a in Figure 6). Decorated by aniline oligomer, the sheet resistivity of MWNT-COOH was decreased to 850 Ω sq^{-1} (Sample b in Figure 6). It was reported that MWNT can dope PANI to be conducting due to the strong π–π interactions, virtually through the formation of a charge–transfer complex by affecting both the free N–H environment and quinoid units along PANI backbone.[33] Therefore, the electrical conductivity of MWNT-COOH was enhanced upon attachment of aniline oligomer. It can be illustrated from the XPS analysis. The N1s core-level spectrum of MWNT-AO was shown in Figure 6(a), which was deconvoluted into three component peaks[34,35] centered at 402.2, 401.1, and 399.6 eV. The peak centered at 402.2 eV can be assigned to the iminium ions (—NH$^+$=) of the conductive PANI units. The peak centered at 401.1 eV is attributed to the radical cation nitrogen and is about 53.4% of the total nitrogen atoms, implying that the doping level is 53.4% in MWNT-AO.[36] From the analysis on the doping level, it showed that quite a number of nitrogen sites along the aniline oligomer could be further doped by the different dopants, such as APE. That is, MWNT-AO doped with APE should have the higher electrical conductivity than MWNT-AO, because of the newly formed conductive pathways. However, the sheet resistivity of solution casting APE/MWNT-AO films was not accordingly decreased. On the contrary, it was increased to 1526 Ω sq^{-1} (Sample c in Figure 6). This is probably because the presence of competition between MWNT and APE for doping aniline oligomer makes a quantity of APE unreacted, which forms the insulating structures in the film.

To further enhance the electrical conductivity, a filtrating process was followed. After removal of the excess unreacted organic dopant, by vacuum filtrating of the APE/MWNT-AO dispersion through a 0.2 μm polycarbonate membrane, the sheet resistivity of the obtained films was significantly decreased to 131 Ω sq^{-1} (Sample d in Figure 6), which has the same order of magnitude as that of the single-walled carbon nanotube (SWNT) films (150–300 Ω sq^{-1}) prepared by using spray coating[37] and vacuum filtering[38] of pristine SWNT dispersion. From the N1s core-level spectrum of the resultant APE/MWNT-AO films shown in Figure 7(b), the content of radical cation nitrogen corresponding to the doping level was increased to 64.7%. That is to say, 11.3% molar ratio of the 16-mer aniline on MWNT-AO was further doped to be conducting by APE after filtrating compared with that of pristine MWNT-AO [Figure 7(a)], from which the actual weight content of APE remained in the as-prepared film is calculated to be 7%. In addition, from the SEM images shown in Figure 8, the MWNTs in APE/MWNT-AO films after filtrated were more evenly and densely connected [Figure 8(b)], in comparison with that of solution casting APE/MWNT-AO films without filtrating [Figure 8(a)], which endowed the system relatively high-mechanical strength and easily releasing behavior from the supporting substrate.

TGA Thermograms

To determine the weight content of MWNTs, TGA of the MWNT-COOH, and the as-prepared MWNT-AO film from

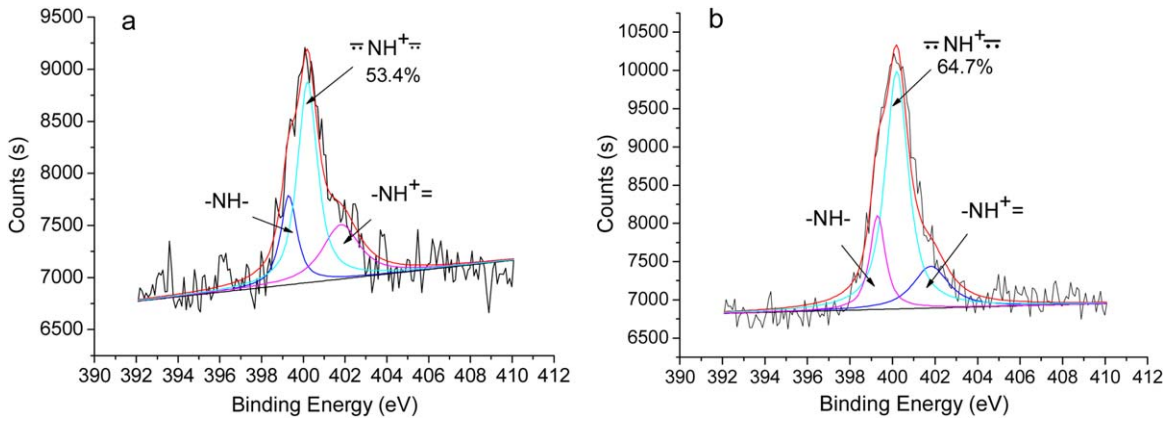

Figure 7. N1s XPS spectra of (**a**) MWNT-AO and (**b**) APE/MWNT-AO films after filtrated. [Color figure can be viewed in the online issue, which is available at wileyonlinelibrary.com.]

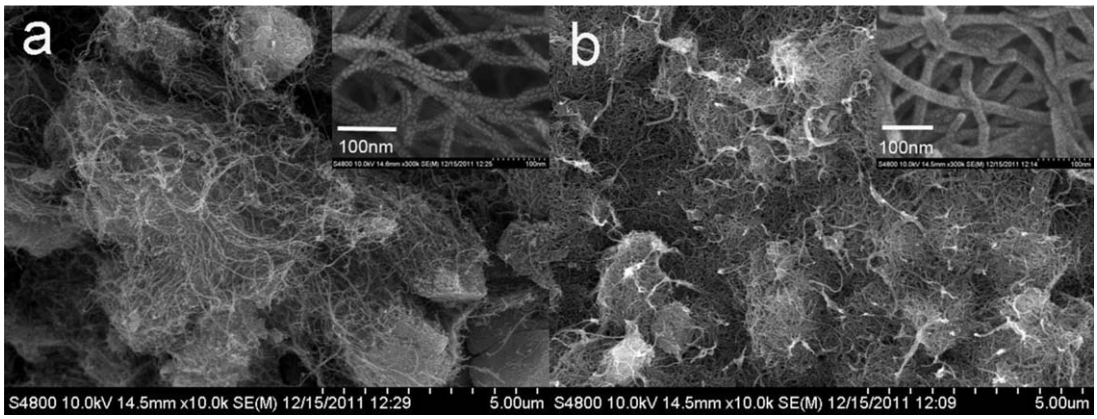

Figure 8. SEM images of (**a**) solution casting APE/MWNT-AO films and (**b**) free-standing APE/MWNT-AO films after filtrated. Inset of (a) and (b) shows the high-resolution image, respectively.

filtrating was carried out at temperatures ranging from room temperature to 800°C under nitrogen. As shown from the weight loss profile of MWNT-COOH in Figure 9(a), there appear to be two typical stages of weight loss beginning at approximately 140°C and approximately 413°C, which might be correspondent to the functional group decomposition of COOH and the sp^2 structures. While only one stage of weight loss beginning at approximately 550°C corresponding to decomposition of the sp^2 structures was found for MWNTs [Figure 9(b)]. This is because the intrinsic sp^2 structures were partially destroyed during the incorporation of the carboxyl groups, which makes the thermal stability of MWNT-COOH deceased compared with that of MWNTs. From the weight loss in Figure 9(a), it can be found the weight content of COOH unit was around 0.5%.

In the case of free-standing APE/MWNT-AO films from filtrating (Figure 10), two typical stages of weight loss beginning at approximately 160°C and approximately 500°C were observed. The weight drop beginning at approximately 160°C and ending at approximately 500°C was resulted from aniline oligomer linked to the surface of MWNTs and the dopant APE contained in the film, whose weight drop beginning is at approximately

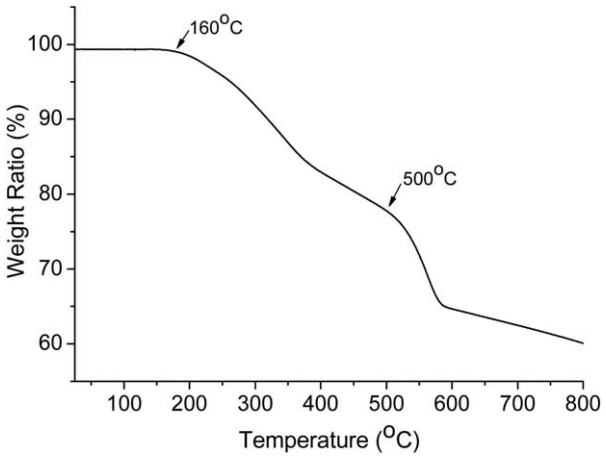

Figure 10. TGA thermograms of the free-standing APE/MWNT-AO films.

140°C and approximately 200°C, respectively (see Figure 11). The second weight loss beginning at approximately 500°C corresponds to the sp^2 structure decomposition of MWNTs. From Figure 10, the weight loss of the first stage was around 23%, which is in good agreement with the total weight content of the 16-mer aniline (16 wt %) calculated from the molar ratio of

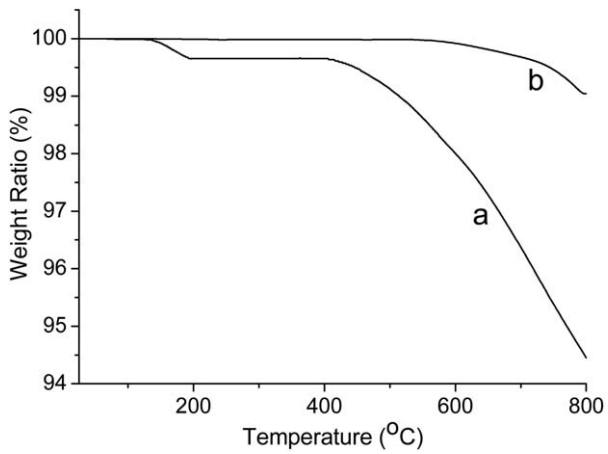

Figure 9. TGA thermograms of (**a**) MWNT-COOH and (**b**) Pristine MWNT.

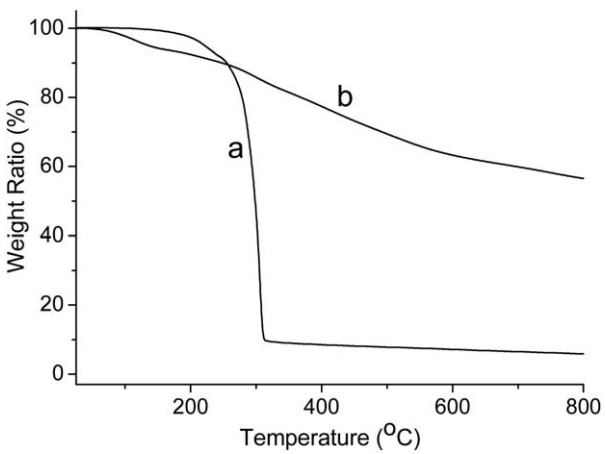

Figure 11. TGA thermograms of (**a**) APE and (**b**) 16-mer aniline.

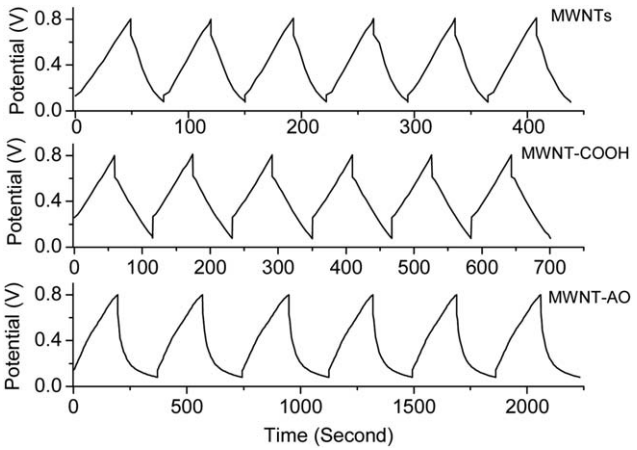

Figure 12. Galvanostatic charge–discharge curves of MWNTs, MWNT-COOH, and APE/MWNT-AO films prepared by filtrating at the current density of 1.0 A g^{-1}.

carboxyl units on MWNTs and the APE (7 wt %) calculated from the XPS data. That is to say, the MWNTs content in the free-standing film can be over than 77%. Such a high-MWNT loading supplied the resultant films higher electrical conductivity.

Capacitance

Because of the high-theoretical specific pseudocapacitance from multiple redox states,[39,40] PANI has been considered as one of the most promising materials. In order to find the effect of aniline oligomer on the capacitance of MWNTs, galvanostatic charge/discharges of the obtained films at high-current densities were measured. Typical galvanostatic charge/discharge curves of the MWNTs, MWNT-COOH, and APE/MWNT-AO electrode in 1*M* H_2SO_4 are presented in Figure 12. All the composite electrodes showed the quasi-triangular shape which is characteristic of electrical double-layer capacitance.[41] Calculated from discharge time, the specific capacitance of neat MWNTs is 43 F g^{-1} at a current density of 1.0 A g^{-1}, and it is 86 F g^{-1} for MWNT-COOH due to the presence of the activated groups of carboxyl, which was reported to show the pseudo-capacitance through a Faradic reaction.[42] However, the specific capacitance was increased to around 249 F g^{-1} for the free-standing APE/MWNT-AO films, which is mainly resulted from the high pseudocapacitance of the PANI units on MWNT. Accompanied by the low-sheet resistivity, this electrochemical active film with a better storage capacity may find its possible application as the electrode materials for electronic devices and supercapacitors.

CONCLUSIONS

High electrochemical active free-standing MWNT films could be easily synthesized from aniline oligomer functionalized MWNTs, by using filtration of APE-doped MWNT-AO dispersions, which showed the sheet resistivity as low as 131 Ω sq^{-1}. The aniline oligomer functionalization of MWNTs and the doping process followed resulted in solubility enhancement of MWNTs. Compared with the MWNT-COOH, the decrease of sheet resistivity of APE/MWNT films was attributed to the doping of aniline oligomer by MWNT and APE, discerned from the XPS data. Additionally, the free-standing films showed both homogeneously distributed and densely packed morphology, which endowed the APE/MWNT automatically releasing from the filter membrane. TGA thermograms showed that the MWNT loading in the as-prepared film can be over than 77%. Encouragingly, this functionalized MWNT film showed the specific capacitance as high as 249 F g^{-1}, mainly resulted from the high pseudocapacitance of the aniline units on MWNT.

ACKNOWLEDGMENTS

This work was financially supported by the National Natural Science Foundation of China (Grant No. 21103133); the Scientific Research Foundation for the Returned Overseas Chinese Scholars, State Education Ministry; the Natural Science Foundation of Shaanxi Province (No. 2013JM6012); Shaanxi Provincial Education Department Program (No.2013JK0928, No.11JK0800); the Open Research Fund Program of Key Laboratory of Photochemical Conversion and Optoelectronic Materials, TIPC, Chinese Academy of Sciences and the National Training Programs of Innovation and Entrepreneurship for Undergraduates (No. 201210702015, No. 201210702017).

REFERENCES

1. Wu, Z. C.; Chen, Z. H.; Du, X.; Logan, J. M.; Sippel, J.; Nikolou, M.; Kamaras, K.; Reynolds, J. R.; Tanner, D. B.; Hebard, A. F.; Rinzler, A. G. *Science* **2004**, *305*(5688), 1273–1276.
2. Gruner, G. *J. Mater. Chem.* **2006**, *16*, 3533–3539.
3. Kim, J.; Hong, A. J.; Chandra, B.; Tulevski, G. S.; Sadana, D. K. *Adv. Mater.* **2012**, *24*(14), 1899–1902.
4. Niu, Z.; Dong, H.; Zhu, B.; Li, J.; Hng, H. H.; Zhou, W.; Chen, X.; Xie, S. *Adv. Mater.* **2013**, *25*(7), 1058–1064.
5. Futaba, D. N.; Hata, K.; Yamada, T.; Hiraoka, T.; Hayamizu, Y.; Kakudate, Y.; Tanaike, O.; Hatori, H.; Yumura, M.; Iijima, S. *Nat. Mater.* **2006**, *5*(12), 987–994.
6. Shaijumon, M. M.; Ou, F. S.; Ci, L. J.; Ajayan, P. M. *Chem. Commun.* **2008**, (*20*), 2373–2375.
7. Bekyarova, E.; Itkis, M. E.; Cabrera, N.; Zhao, B.; Yu, A. P.; Gao, J. B.; Haddon, R. C. *J. Am. Chem. Soc.* **2005**, *127*(16), 5990–5995.
8. Tenent, R. C.; Barnes, T. M.; Bergeson, J. D.; Ferguson, A. J.; To, B.; Gedvilas, L. M.; Heben, M. J.; Blackburn, J. L. *Adv. Mater.* **2009**, *21*, 3210–3216.
9. Hall, L. J.; Coluci, V. R.; Galvao, D. S.; Kozlov, M. E.; Zhang, M.; Dantas, S. O.; Baughman, R. H. *Science* **2008**, *320*(5875), 504–507.
10. Nasibulin, A. G.; Kaskela, A. O.; Mustonen, K.; Anisimov, A. S.; Ruiz, V.; Kivistö, S.; Rackauskas, S.; Timmermans, M. Y.; Pudas, M.; Aitchison, B.; Kauppinen, M.; Brown, D. P.; Okhotnikov, O. G.; Kauppinen, E. I. *ACS Nano* **2011**, *5*(4), 3214–3221.
11. Noerochim, L.; Wang, J.; Chou, S.; Wexler, D.; Liu, H. *Carbon* **2012**, *50*(3), 1289–1297.
12. Wang, Q. G.; Liu, N. J.; Wang, X. H.; Li, J.; Zhao, X. J.; Wang, F. S. *Macromolecules* **2003**, *36*, 5760–5764.

13. Luo, J.; Jiang, S.; Wu, Y.; Chen, M.; Liu, X. *J. Polym. Sci. Part A: Polym. Chem.* **2012**, *50*(23), 4888–4894.
14. Salaneck, W. R.; Lundström, I.; Huang, W. S.; MacDiarmid, A. G. *Synth. Met.* **1986**, *13*, 291–297.
15. Cao, Y.; Smith, P.; Heeger, A. *J. Synth. Met.* **1992**, *48*, 91–97.
16. Sainz, R.; Benito, A. M.; Martinez, M. T.; Galindo, J. F.; Sotres, J.; Baro, A. M.; Corraze, B.; Chauvet, O.; Maser, W. K. *Adv. Mater.* **2005**, *17*(3), 278–281.
17. Feng, W.; Bai, X. D.; Lian, Y. Q.; Liang, J.; Wang, X. G.; Yoshino, K. *Carbon* **2003**, *41*(8), 1551–1557.
18. Jiménez, P.; Castell, P.; Sainz, R.; Ansón, A.; Martínez, M. T.; Benito, A. M.; Maser, W. K. *J. Phys. Chem. B* **2010**, *114*(4), 1579–1585.
19. Jiménez, P.; Maser, W. K.; Castell, P.; Martínez, M. T.; Benito, A. M. *Macromol. Rapid Commun.* **2009**, *30*(6), 418–422.
20. Jeon, I.; Kang, S.; Tan, L.; Baek, J. *J. Polym. Sci. Part A: Polym. Chem.* **2010**, *48*(14), 3103–3112.
21. Zhao, B.; Hu, H.; Haddon, R. C. *Adv. Funct. Mater.* **2004**, *14*(1), 71–76.
22. White, C. T.; Todorov, T. N. *Nature* **1998**, *393*, 240–242.
23. Wang, K.; Wang, Y.; Wang, Y.; Hosono, E.; Zhou, H. *J. Phys. Chem. C* **2009**, *113*(3), 1093–1097.
24. Frackowiak, E.; Béguin, F. *Carbon* **2002**, *40*, 1775–1787.
25. Stejskal, J.; Sapurina, I.; Trchová, M.; Konyushenko, E. N.; Holler, P. *Polymer* **2006**, *47*, 8253–8262.
26. Zhang, W. J.; Feng, J.; MacDiarmid, A. G.; Epstein, A. *J. Synth. Met.* **1997**, *84*(1-3), 119–120.
27. Liu, J.; Rinzler, A. G.; Dai, H.; Hafner, J. H.; Bradley, R. K.; Boul, P. J.; Lu, A.; Iverson, T.; Shelimov, K.; Huffman, C. B.; Rodriguez-Macias, F.; Shon, Y. S.; Lee, T. R.; Colbert, D. T.; Smalley, R. E. *Science* **1998**, *280*(5367), 1253–1256.
28. Diao, P.; Liu, Z. F.; Wu, B.; Nan, X. L.; Zhang, J.; Wei, Z. *Chem. Phys. Chem.* **2002**, *3*, 898–901.
29. Hong, S. Y.; Tobias, G.; Ballesteros, B.; El Oualid, F.; Errey, J. C.; Doores, K. J.; Kirkland, A. I.; Nellist, P. D.; Green, M. L. H.; Davis, B. G. *J. Am. Chem. Soc.* **2007**, *129*(36), 10966–10967.
30. Sainsbury, T.; Fitzmaurice, D. *Chem. Mater.* **2004**, *16*, 3780–3790.
31. Han, J.; Song, G. P.; Guo, R. *J. Polym. Sci. Part A: Polym. Chem.* **2006**, *44*, 4229–4234.
32. Cao, A.; Xu, C.; Liang, J.; Wu, D.; Wei, B. *Chem. Phys. Lett.* **2001**, *344*(1-2), 13–17.
33. Zengin, H.; Zhou, W.; Jin, J.; Czerw, R.; Smith Jr., D. W.; Echegoyen, L.; Caroll, D.; Foulger, S.; Ballato, *J. Adv. Mater.* **2002**, *14*, 1480–1483.
34. Chen, S. A.; Hwang, G. W. *J. Am. Chem. Soc.* **1995**, *117*, 10055–10062.
35. Wei, X. L.; Fahlman, M.; Epstein, A. *J. Macromolecules* **1999**, *32*(9), 3114–3117.
36. Wang, Q. G.; Wang, X. H.; Li, J.; Zhao, X. J.; Wang, F. S. *Synth. Met.* **2005**, *148*, 127–132.
37. Liu, Q. F.; Fujigaya, T.; Cheng, H. M.; Nakashima, N. *J. Am. Chem. Soc.* **2010**, *132*(46), 16581–16586.
38. Shi, Z.; Chen, X.; Wang, X.; Zhang, T.; Jin, *J. Adv. Funct. Mater.* **2011**, *21*, 4358–4363.
39. Lu, J.; Moon, K. S.; Kim, B. K.; Wong, C. P. *Polymer* **2007**, *48*(6), 1510–1516.
40. Mirmohseni, A.; Dorraji, M. S. S.; Hosseini, M. G. *Electrochim. Acta* **2012**, *70*, 182–192.
41. Lei, Z. B.; Chen, Z. W.; Zhao, X. S. *J. Phys. Chem. C* **2010**, *114*, 19867–19874.
42. Li, L.; Li, F. *New Carbon Mater.* **2011**, *26*(3), 224–228.